CROSS-DIFFUSION EFFECTS ON HEAT AND MASS TRANSFER OF MAGNETOHYDRODYNAMICS FLOW IN POROUS MEDIA OVER EXPONENTIALLY STRETCHING SURFACE

Supported by tetfund TERTIARY EDUCATION TRUST FUND

S. A. Amoo[1] and A. S. Idowu[2]
[1]Department of Mathematics and Statistics, Federal University Wukari, Taraba State, Nigeria
[2]Department of Mathematics, University of Ilorin, Kwara State, Nigeria

Received: December 13, 2017 **Accepted:** August 19, 2018

Abstract: Magnetohydrodynamics (MHD) boundary layer fluid flow in a porous medium over exponentially stretching sheet in the presence of heat generation and chemical reaction is the thrust of this paper. The study investigated the effects of Dufour (diffusion-thermo) and Soret (thermo-diffusion) on heat and mass transfer of MHD fluid flow in porous media over stretching surface. The PDEs were reduced to a coupled nonlinear Ordinary Differential Equations (ODEs) using similarity transformations. The ODEs representing the fluid flow, convective heat and mass transfer were simplified and solved by fourth order Runge-Kutta method with shooting technique. The result showed that: increase in Df and Sr. effects led to increase in skin friction but decrease was Sherwood and Nusselt respectively whereas decrease in Nusselt was noticed in the case of Dufour effect but increase was noticed in the case of Soret effect. Increase in radiation parameter led to corresponding increase in skin friction and Sherwood numbers but not in Nusselt number. The study concluded that solutal Grashof, thermal Grashof, magnetic parameter, radiation parameter, Dufour and Soret numbers had significant effects on MHD fluid flow in porous media stretching surface. This study is recommended for use in plastic extrusion as well as MHD power generation systems.

Keywords: Cross-diffusion, Magnetohydrodynamics, Dufour, Soret numbers

Introduction

The significance of cross-diffusion effects on heat and mass transfer of MHD flow in porous media over exponentially stretching porous surface had been subject of discussion among the researchers due to its applications in industries and environment issues. Several authors like Shankar (2010), Sinivasacharya and RamReddy (2012, 2013), Nalinashi (2013), Ali and Alam (2014) had discussed about significance of cross-diffusion effects and the associated MHD fluid flow. Why this significance? The researchers' attention to cross-diffusion was borne out of the usefulness of the outcome of such research in explaining boundary layer theories as it affects convective MHD fluid flow systems. It is a well-known phenomenon that fluids including oil, water, and ethylene glycol are poor conductors of heat. Since the thermal conductivity of these fluids play important roles on the heat transfer coefficient between medium and the surface; studying cross-diffusion heat transfer between them is very important.

Specifically, the authors such as Subhakar and Gangadhar (2012), Sharma, Prasad, Govardhan (2013), Srinivasa, Charya and Upendar (2014) had realized and discovered that the flow of ground water through soil and rocks (porous media) is very important for agriculture and pollution control; extraction of oil and natural gas from rocks which are prominent in oil and naturally gas industry; functioning of muscles in body (bone, cartilage and muscle and so on) belong to porous media. Flow of blood and treatments through them; understanding various medical conditions (such as tumor growth, a formation of porous media) and their treatment (such as injection, a flow through porous media in medical sciences). Irogham and Pop (2005), Vafai (2005), Nield and Bejan (2006), Vadasz (2008) and Sharman *et al.* (2013) stated that heat and mass transfer by free convection in porous media have wide applications in engineering such as post accidental heat removal in nuclear reactors, solar collectors, drying processes, geothermal and oil recovery.

On the other hand, according to Sibanda, Khidir and Awad (2012), convection driven by two different fluid components which have different rates of diffusion play a great role in fluid dynamics since such flows occur naturally in many physical and engineering processes. For example, heat and salt in the sea water provide the best known example of double diffusive convection. Sharma *et al.* (2013) studied two dimensional steady free convection and mass transfer flow past a continuously moving semi-infinite vertical porous plate in porous medium. Sibanda *et al.* (2012) investigated cross-diffusion effects on flow over a vertical surface using linearization method. Alarbi, Bazid and El Gendy (2010) studied heat and mass transfer in MHD visco-elastic fluid flow through a porous medium over a stretching sheet with chemical and thermal stratification effects.

On the other hand, Subhakar and Gangadhar (2012) investigated the combined effect of the free convective heat and mass transfer on the unsteady two boundary layer flow over a stretching vertical plate in the presence of heat generation/absorption. In some book and research studies, Bergman *et al.* (2011), Subhakar and Gangadhar (2012) reported that Dufour and Soret effects were often neglected since they are of smaller order of magnitude than the effects described by Fourier's and Fick's laws. When the heat and mass transfer occur simultaneously in a moving fluid, the relations between the fluxes and driving potentials are more complicated. It was found that an energy flux can be generated not only by the temperature gradients but also by the composition gradients. The mass transfer caused by thermal gradient is also called Soret effects while the heat transfer caused by the concentration gradient is called Dufour effect. Meanwhile such effects become crucial when the density difference exists in the flow regimes. The Soret effect, for example has been utilized for isotope separation. In a mixture between gases with very light molecular weight (He, $H2O$) and medium molecular weight ($N2$, air), the Dufour effect was found to be of considerable magnitude such that it cannot be neglected (Eckert and Drake, 1972). Cross-diffusion is used as Soret or thermal-diffusion and Dufour or diffusion-thermal. This arrangement involves the use of Soret in temperature and Dufour in concentration and by alternating the terms means cross-diffusion.

Thermal-diffusion also refers to as thermo-diffusion or Soret effect that corresponds to species differentiation developed in

an initial homogeneous mixture subjected to a temperature gradient. The heat flux induced by a concentration gradient is called Dufour or diffusion-thermo effect. After review of literature, the present study examined the cross-diffusion effects on heat and mass transfer of MHD in porous media over exponentially stretching surface.

Formulation of the Problem

Consider the thermal radiation effect on free convective heat and mass transfer of MHD flow of an electrically conducting, steady and incompressible fluid flow past an exponentially stretching sheet under the action of thermal and solutal buoyancy forces. A uniform transverse variable magnetic field $B(x)$ is applied perpendicular to the direction of flow with chemical reaction is taking place in the fluid flow. The transverse applied magnetic field and induced magnetic are assumed to be very small, so that the induced magnetic field is negligible. The flow is assumed to be in the x-direction with y-axis normal to it. The flow of an incompressible and radiating fluid near an impermeable vertical sheet stretching with velocity $Uw(x)$, temperature distribution $Tw(x)$ and concentration distribution $Cw(x)$ moving through a quiescent ambient fluid of constant temperature $T1$ and concentration $C1$ were considered. The presence of thermal diffusion (Soret) and diffusion-thermo (Dufour) effects were included. A uniform magnetic fluid was applied in the direction perpendicular or normal to the stretching surface. The plate is maintained at the temperature and species concentration Tw, Cw and free stream temperature and species concentration $T1$, $C1$, respectively. The geometry of the model and equations governing the cross-diffusion effects of heat and convective mass transfer of MHD fluid flow in a porous medium over exponentially stretching sheet are detailed. The schematic diagram of the problem is shown in the geometry of the model and coordinate system, Fig. 1.

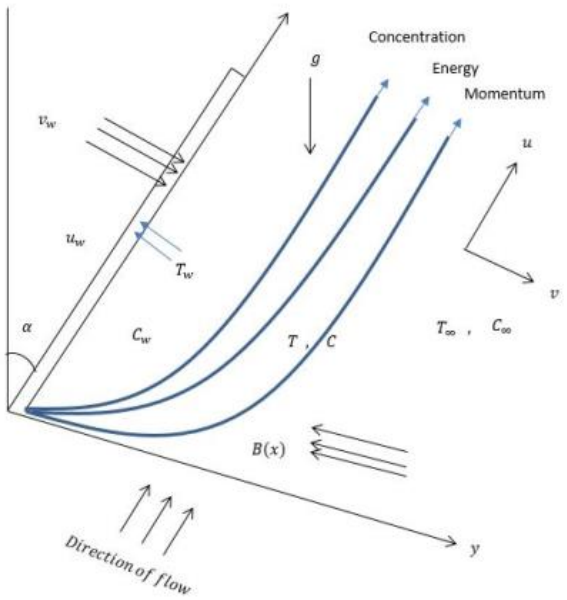

Fig. 1: The geometry of the model and coordinate system

Continuity equation

$$\frac{\partial u}{\partial x}+\frac{\partial v}{\partial y}=0 \qquad (1)$$

Momentum equation

$$u\frac{\partial u}{\partial x}+v\frac{\partial u}{\partial y}=-\frac{1}{\rho}\sigma B_0{}^2(x)u+\nu\frac{\partial^2 u}{\partial y^2}+g\beta_T\left(T-T_\infty\right)\cos(\alpha)+g\beta_C\left(C-C_\infty\right)\cos(\alpha)-\frac{\nu}{K}u \qquad (2)$$

Energy equation

$$\rho C_p\left(u\frac{\partial T}{\partial x}+v\frac{\partial T}{\partial y}\right)=k\frac{\partial^2 T}{\partial y^2}-\frac{\partial q_r}{\partial y}+Q_0\left(T-T_\infty\right)+\frac{D_m\partial^2 C}{C_s\partial y^2} \qquad (3)$$

Concentration equation

$$u\frac{\partial C}{\partial x}+v\frac{\partial C}{\partial y}=D\frac{\partial^2 C}{\partial y^2}-\gamma\left(C-C_\infty\right)+\frac{D_m\partial^2 T}{T_m\partial y^2} \qquad (4)$$

Subject to the following boundary conditions:

$$u=U_0e^{\frac{x}{L}},v=-V_0e^{\frac{x}{L}},T=T_w=T_\infty+T_0e^{\frac{x}{2L}},C=C_w=C_\infty+C_0e^{\frac{x}{2L}}\ \ at\ \ y=0$$
$$u\to 0,T\to T_\infty,C\to C_\infty\ \ as\ \ y\to\infty \qquad (5)$$

where u and v velocity component in the x direction, velocity component in the y direction C, and T are concentration of the fluid species and fluid temperature respectively. L is the reference length, $B(x)$ is the magnetic field strength, U_0 is the reference velocity and V_0 is the permeability of the porous surface. The physical quantities K; ρ, ν, σ, D, k, C_p, Q_0, γ, Cs , T_m and K_T are the permeability of the porous medium, density, fluid kinematics viscosity, electric conductivity of the fluid, coefficient of mass diffusivity, thermal conductivity of the fluid, specific heat capacity at constant pressure, rate of specific internal heat generation or absorption, reaction rate coefficient, concentration susceptibility and mean fluid temperature, and thermal diffusion ratio respectively. G is the gravitational acceleration; the last terms of equations (3) and (4) are Dufour or diffusion thermo effect and the Soret or thermo-diffusion effect. β_T and β_C are the thermal and mass expansion coefficients respectively. q_r is the radiative heat flux in the y direction. By using the Rosseland approximation according to Ibrahim and Suneetha (2015), the radiative heat flux q_r is given by;

$$q_r=-\frac{4\sigma_0}{3\delta}\frac{\partial T^4}{\partial y} \qquad (6)$$

where σ_0 and δ are the Stefan-Boltzmann constant and the mean absorption coefficient respectively. Assume the temperature difference within the flow is sufficiently small such that T^4 may be expressed as a linear function of temperature, using Taylor series to expand T^4 about the free stream T_∞ and neglecting higher order terms, this gives the approximation;

$$T^4 \cong 4T_\infty^3 T - 3T_\infty^4 \qquad (7)$$

Following from equations (6) and (7), equation (3) becomes:

$$\left(u\frac{\partial T}{\partial x} + v\frac{\partial T}{\partial y}\right) = \left(\frac{k}{\rho C_p} + \frac{16\sigma_0 T_\infty^3}{3\rho C_p \delta}\right)\frac{\partial^2 T}{\partial y^2} + \frac{Q_0}{\rho C_p}(T - T_\infty) + \frac{D_m \partial^2 T}{C_s \partial y^2} \qquad (8)$$

The magnetic field $B(x)$ is assumed to be in the form

$$B(x) = B_0 e^{\frac{x}{2L}} \qquad (9)$$

where B_0 is the constant magnetic field. Introducing the stream function (x, y) such that:

$$u = \frac{\partial \psi}{\partial y}, \quad v = -\frac{\partial \psi}{\partial x}, \qquad (10)$$

Using equation (10) in equations (1), (2), (4) and (8), the continuity equation is satisfied; then equations (2), (4) and (8) become:

$$\frac{\partial \psi}{\partial y}\frac{\partial^2 \psi}{\partial x \partial y} - \frac{\partial \psi}{\partial x}\frac{\partial^2 \psi}{\partial y^2} = -\frac{\sigma}{\rho}B_0 e^{\frac{x}{2L}}\left(\frac{\partial \psi}{\partial y}\right) + \nu\frac{\partial^3 \psi}{\partial y^3} + g\beta_T(T - T_\infty)\cos(\alpha) + g\beta_C(C - C_\infty)\cos(\alpha) - \frac{\nu}{K}\left(\frac{\partial \psi}{\partial y}\right) \qquad (11)$$

$$\frac{\partial \psi}{\partial y}\frac{\partial T}{\partial x} - \frac{\partial \psi}{\partial x}\frac{\partial T}{\partial y} = \left(\frac{k}{\rho C_p} + \frac{16\sigma_0 T_\infty^3}{3\rho C_p \delta}\right)\frac{\partial^2 T}{\partial y^2} + \frac{Q_0}{\rho C_p}(T - T_\infty) + \frac{D_m \partial^2 C}{C_s \partial y^2} \qquad (12)$$

$$\frac{\partial \psi}{\partial y}\frac{\partial C}{\partial x} - \frac{\partial \psi}{\partial x}\frac{\partial C}{\partial y} = D\frac{\partial^2 C}{\partial y^2} - \gamma(C - C_\infty) + \frac{D_m \partial^2 T}{T_m \partial y^2} \qquad (13)$$

The corresponding boundary conditions become:

$$\frac{\partial \psi}{\partial y} = U_0 e^{\frac{x}{L}}, \frac{\partial \psi}{\partial x} = V_0 e^{\frac{x}{L}}, T = T_w = T_\infty + T_0 e^{\frac{x}{2L}},$$
$$C = C_w = C_\infty + C_0 e^{\frac{x}{2L}} \quad at \quad y = 0 \qquad (14)$$
$$\frac{\partial \psi}{\partial y} \to 0, T \to T_\infty, C \to C_\infty \quad as \quad y \to \infty$$

In this study, similarity variables (15) can be applied

$$\psi(x, y) = \sqrt{2\nu U_0 L}e^{\frac{x}{2L}} f(\eta), \eta = y\sqrt{\frac{U_0}{2\nu L}}e^{\frac{x}{2L}}, T = T_\infty + T_0 e^{\frac{x}{2L}}\theta(\eta), \qquad (15)$$
$$C = C_\infty + C_0 e^{\frac{x}{2L}}\phi(\eta)$$

In view of the similarity variable (15) on equations (11) to (14), according to (Sajid and Hayat, 2008; Amoo and Idowu, 2017), the following nonlinear equations (16) to (18) were obtained;

$$f''' + ff'' - 2f'^2 - (M + D_a)f' + G_r\theta\cos(\alpha) + G_c\phi\cos(\alpha) = 0 \qquad (16)$$

$$\left(1 + \frac{4}{3}R\right)\theta'' + P_r(f\theta' - f'\theta + Q\theta + D_f\phi'') = 0 \qquad (17)$$

$$\phi'' + S_c(f\phi' - f'\phi - \lambda\phi + S_r\theta'') = 0 \qquad (18)$$

Where corresponding boundary conditions take the form equation (19):

$$f = f_w, f' = 1, \theta = 1, \phi = 1 \ \ at \ \ \eta = 0$$
$$f' = 0, \theta = 0, \phi = 0 \ \ as \ \ \eta \to \infty \qquad (19)$$

where α is the angle of inclination, $M = \frac{2\sigma LB_0}{\rho U_0} e^{\frac{x}{2L}}$ is the magnetic parameter, $Da = \frac{2\nu L}{U_0 K} e^{-\frac{x}{L}}$ is the Darcy porosity parameter, $Gc = \frac{2Lg\beta_T T_0}{U_0^2} e^{-\frac{3x}{2L}}$ is the thermal Grashof number, $Gc = \frac{2Lg\beta_C C_0}{U_0^2} e^{-\frac{3x}{2L}}$ is the solutal Grashof number, $\Pr = \frac{\rho\nu C_p}{k}$ is the Prandtl number, $R = \frac{4\sigma_0 T_\infty^3}{\delta k}$ is the thermal radiation parameter, $Q = \frac{2LQ_0}{U_0 \rho C_p} e^{-\frac{x}{L}}$ is the heat generation parameter, $Sc = \frac{\nu}{D}$ is the Schmidt number, $\lambda = \frac{2L\gamma}{U_0} e^{-\frac{x}{L}}$ is the chemical reaction parameter, $f_w = V_0 \sqrt{\frac{2L}{\nu U_0}} e^{-\frac{3x}{2L}}$ is the permeability of the plate, $D_f = \frac{D_m U_0}{C_s 2\nu L} C_0 e^{\frac{3x}{2L}} \phi''$ is Dufour parameter and $S_r = \frac{D_m U_0}{T_m 2\nu L} T_0 e^{\frac{3x}{2L}} \theta''$ is Soret parameter.

Methodof solution

The governing equations of convection, cross-diffusion convective heat and mass transfer in fluids are essentially nonlinear ordinary differential equations. Hence, the system of nonlinear ODEs together with the boundary conditions are solved numerically using fourth order Runge-Kutta scheme with shooting technique. The method has been proven to be adequate for boundary layer equations, seems to give accurate results and has been widely used (Ibrahim and Makinde, 2010). It seems to be the most flexible of the common methods. The scheme is also applicable to various types of boundary layer flow problems including the free and mixed connection flows. In the numerical method employed in solving the models equations i.e. the boundary valued problems (BPV).Shooting method reformulates the BVP to IVP by adding sufficient number of conditions at one end and adjust these conditions until the given conditions are satisfied at the other end while Runge-Kutta method solve the initial value problems.

Equations (16) - (19) were integrated as IVPs, the values for f ‘’’(0), θ’(0) and φ’(0) which were required to explain skin friction, Nusselt and Sherwood numbers, but no such values were given at the boundary. The suitable guess values for f ‘’(0) , θ’(0)and φ’(0) were chosen and then integration was carried out. The researchers compared the calculated values for f’’(0), θ’(0) and φ’(0) at η = 7 with the given boundary conditions f’’(7) = 0, θ’(7) = 0 and φ’(7) = 0. Then adjusted the estimated values for f’’(0) , θ’(0) and φ’(0), to give a better approximation for the solution. The researcher performed series of computations to obtain values for f’’(0), θ’(0) and φ’(0), and then applied a fourth order Runge-Kutta method with shooting technique with step-size h = 0.01. The above procedure was repeated until the results up to the desired degree of accuracy 10^{-6}.

The numerical computation to obtain velocity, temperature and concentration profiles were presented. The effect of the computation on heat and free convective mass transfer as well as proportional effects on the skin friction coefficient, Nusselt number and local Sherwood number are presented and examined for different values of the independent parameters. These enabled the researcher to use the effects of dimensionless parameters to explain cross-diffusion on free convective heat and mass transfer of MHD flow in porous media. However, the physical quantity of practical interest are the local skin friction, the Nussett number *Nu* and local Sherwood number *Sh* defined respectively as:

$$C_f = \frac{\tau_w}{\rho u_w^2}, \quad Nu = \frac{q_w x}{k(T_w - T_\infty)}, \quad Sh = \frac{q_m x}{D_m(C_w - C_\infty)}$$

Where *k* is the thermal conductivity of the fluid, *τw*, *qw* and *qm* are respectively given as;

$$\tau_w = \mu \left(\frac{\partial u}{\partial y}\right)_{y=0}, \quad q_w = k \left(\frac{\partial T}{\partial y}\right)_{y=0}, \quad q_m = D \left(\frac{\partial T}{\partial y}\right)_{y=0}$$

Therefore, the local skin friction coefficient, local Nusselt number and local Sherwood are:

$$C_f Re_x^{\frac{1}{2}} = f''(0), \quad Nu Re_x^{-\frac{1}{2}} = \theta'(0) \quad \text{and} \quad Sh Re_x^{-\frac{1}{2}} = \phi'(0)$$

Where $\mathrm{Re}_x^{\frac{1}{2}} = \frac{U_w x}{\upsilon}$ is the local Reynolds number.

Therefore, *Cf*, *Nu* and *Sh* were rewritten respectively as:

$$C_f \left(\frac{U_w x}{v}\right)^{\frac{1}{2}} = f''(0), \quad Nu \left(\frac{U_w x}{v}\right)^{-\frac{1}{2}} = \theta'(0) \quad \text{and} \quad Sh \left(\frac{U_w x}{v}\right)^{-\frac{1}{2}} = \phi'(0)$$

Results and Discussion

Table 1: Numerical values of θ’(0) and φ’(0) at the sheet for different values of *Gr*, *Gc*,*M*, *fw* and *Sc* when other parameters were made zero was done to validate our result. The comparison of the result of the present study with that of Ibrahim and Makinde (2010) and Lakshmi *et al.* (2012) is presented in Table 1. From Table 1, it could be deduced that the variations of Gr. =Gc. = M = *fw*= 0.1 for numerical values of θ’(0) and φ’(0) at the sheet when compared with the existing literature were in close agreement. The present study had higher values than those of previous studies. A comparison of the previous studies over years had been improvement for Gr = Gc= M= *fw* =0.1 and the present study followed the same trends of improved results. The possible reasons for the trends in variation might be due to accuracy of the method of solution and system of equations or models considered.

The following parameter values were adopted for computation as default values: *M* = 1, *Gr* = 3:5, *Gc* = 2, *fw* = 1, *Q* = 0:5, *R* = 0:5, *Sc* = 0:35, *P r* = 1, *Df* = 0:02, *Sr* = 0:035, α = 0, λ = 0:5. All the computations were carried out using the values in the table except otherwise indicated on the graph.

Table: The comparison of this research with the previous studies for different values of Gr, Gc, M, Fw and Sr

G_r	G_c	M	F_w	S_c	Present study		Lakshmi *et al.* (2012)		Ibrahim and Makinde (2010)	
					$\theta'(0)$	$\phi'(0)$	$\theta'(0)$	$\phi'(0)$	$\theta'(0)$	$\phi'(0)$
0.1	0.1	0.1	0.1	0.62	0.80508	0.74019	0.79904	0.728481	0.79655	0.72533
0.5	0.1	0.1	0.1	0.62	0.84101	0.77380	0.83593	0.76248	0.837901	0.76580
1.0	0.1	0.1	0.1	0.62	0.87617	0.806773	0.87297	0.79681	0.87528	0.80200
0.1	0.5	0.1	0.1	0.62	0.843609	0.776285	0.83850	0.76491	0.84214	0.77017
0.1	0.1	0.1	0.1	0.78	0.803798	0.84118	0.79369	0.83297	0.79369	0.83398

Table 2: Effects of *M, R, Sc; Pr, Da* and λ on $f''(0)$, $\theta'(0)$ and $\varphi'(0)$ (P-parameters)

P	Values	$f''(0)$	$-\theta'(0)$	$-\phi'(0)$	P	Values	$f''(0)$	$-\theta'(0)$	$-\phi'(0)$
M	1	1.24514	0.39613	1.4924	Da	0.001	1.24469	0.39608	1.49423
	3	0.44726	0.31335	1.45824		1	0.82543	0.35328	1.47495
	5	-0.21140	0.24111	1.43103		2.5	0.27147	0.29438	1.45072
	7	-0.77186	0.15951	1.40201		3.5	0.05723	0.25830	1.43712
Gc	2	0.04538	0.30497	1.44762	Gr	3.5	0.30121	0.29662	1.45218
	5	0.82543	0.35328	1.47495		5	0.82543	0.35328	1.47494
	7	1.33214	0.38199	1.49214		7	1.48895	0.41095	1.50274
	10	2.07441	0.42079	1.51656		10	2.42981	0.47654	1.53991
Fw	1	0.82543	0.35328	1.47494	α	15 0	-7.03780	3.06284	-1.70787
	2	0.40849	0.44717	1.85258		30 0	-2.01135	-0.10295	1.37234
	3	0.25750	0.57423	2.26665		45 0	-0.66789	0.19862	1.41467
	4	-1.14774	0.72692	2.71341		75 0	0.59016	0.35328	1.47495
R	0.5	0.82543	0.35328	1.47495	Q	0.5	0.82543	0.35328	1.47495
	1.7	0.93242	0.26609	1.50432		1.5	1.14342	0.29626	1.66824
	3.0	2.11812	-2.29856	2.18338		2.5	1.00851	-1.18601	2.03431
	5.0	4.17894	-7.44577	3.30693		3.5	1.19341	-4.16121	2.56401
Pr.	1.0	0.76205	0.41389	1.45499	Df.	0.2	0.67945	0.75709	1.35120
	2.0	0.61596	0.61186	1.38989		1	0.82543	0.35328	1.47495
	3.0	0.52719	0.85542	1.31448		2	1.01651	0.27821	1.66398
	4.0	0.46235	1.33690	1.16649		4	1.45712	-2.38790	2.28851
Sc.	0.35	0.95553	0.57814	0.98542	λ	0.5	0.82543	0.35328	1.47495
	0.62	0.82543	0.35328	1.47495		1.5	0.76417	0.22381	1.76148
	1.50	0.57988	0.40466	3.20907		2.5	0.71931	0.11749	1.99926
	2.00	0.48787	0.97931	4.54007		4.0	0.66874	0.01685	2.30221
Sr.	0.035	0.80745	0.33884	1.49102					
	0.5	0.82543	0.35328	1.47495					
	1	0.84801	0.36942	1.45413					
	2	0.90491	0.40531	1.39789					

Table 2 represents the numerical analysis of variation independent parameters (magnetic parameter, Darcy parameter, thermal Grashof number, Prandtl number, thermal radiation, and heat generation parameter, Schmidt number and chemical reaction, permeability of the plate surface, Sorest and Dufour parameters) in explaining dependent parameters of Skin friction coefficient, Nusselt and Sherwood numbers at the surface. These further explain exponential analysis of velocity, temperature and concentration profiles thereby showing the effect of cross-diffusion on heat and mass transfer of MHDflow in porous media with suction/injection. All listed parameters are of physical and engineering interest. It was seen from the results that an increase in the values of *M* , *Da* , *fw*, *α*, *Sc* ,Pr. and λ decrease the flow boundary layer while increase in *Gc*, *Gr*. *R. Q. Df* and *Sr*, increase the flow boundary layer. The table depicts that an increase in the values of *M*, *Da, α*, *Q*, *Sc.* and λ thicken the thermal boundary layer by reducing the rate at which heat diffuse out of the system as well as chemical reaction. The increase in *fw* and Pr. reduce the thickness of the thermal boundary layer. It was also discovered that, increase in *fw* , *Q* , *Sc* , *R* and λ cause thinning in the concentration boundary layer while *M* , *Da* and *Pr*. thickened the mass boundary layer. Increase in Dufour and Soret *Sr*. parameters increase the flow at the boundary layer. It means that cross-diffusion parameter effect cannot be totally neglected at the boundary layer phenomena, hence, the significance of cross-diffusion.

Figures 2, 3 and 4 present the effects of magnetic field parameter on fluid flow or velocity, temperature and concentration profiles respectively. It was discovered in Fig. 2 that increases in M slow down the rate of fluid flow thereby thinning the velocity boundary layer. Figs. 3 and 4 represent the distribution of temperature and concentration when the magnetic field parameter was varied. It was discovered that temperature and chemical reaction parameter or concentration decreased. In this case, temperature and concentration at the boundary layer get thinner as magnetic field increased. Figs. 5, 6 and 7 present the effects of exponential velocity, temperature and specie when Darcy porosity was varied. It was discovered that increase in *Da* led to decrease in fluid velocity but increase in temperature and concentration profiles. There were distinct changes observed in momentum and thermal boundary layers while minute changes occurred in concentration boundary layer when Darcy porosity parameters were varied. This result probably follow the convectional flow where both shear layer, thermal and boundary layer have similar characteristics but in cases where heat transfer is influenced by conduction or radiation. The boundary layer for the velocity, temperature profile and concentration exhibited varied behavour.

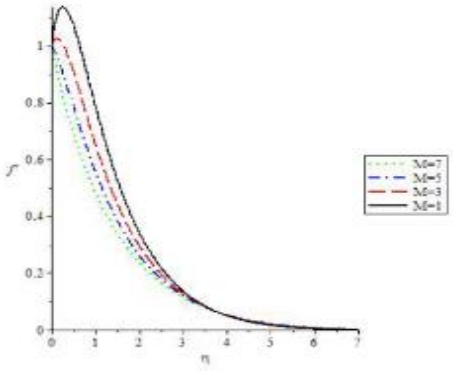

Figure 2: Velocity profile for various values of M

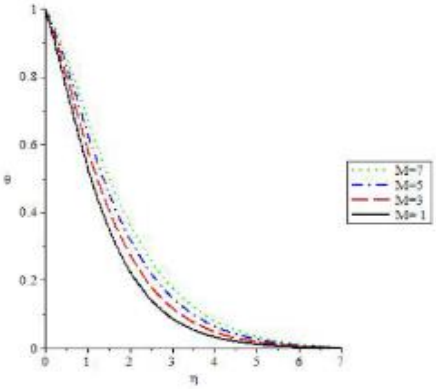

Figure 3: Temperature profile for various values of M

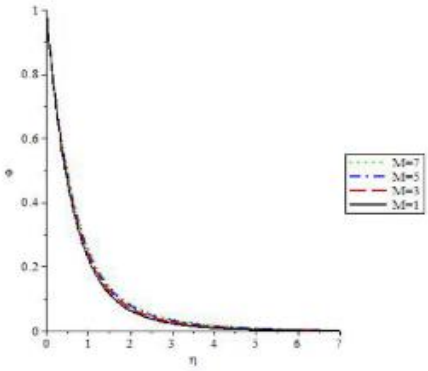

Figure 4: Concentration profile for various values of M

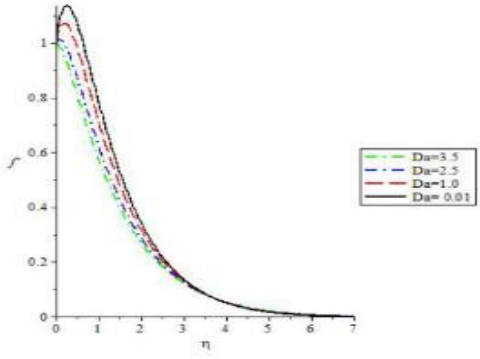

Figure 5: Velocity profile for various values of Da

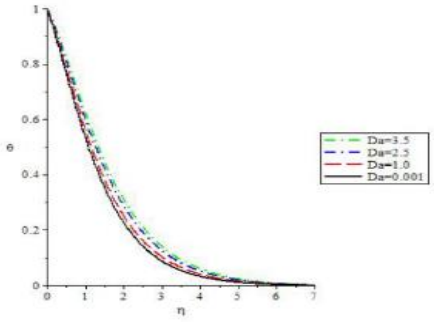

Figure 6: Temperature profile for various values of Da

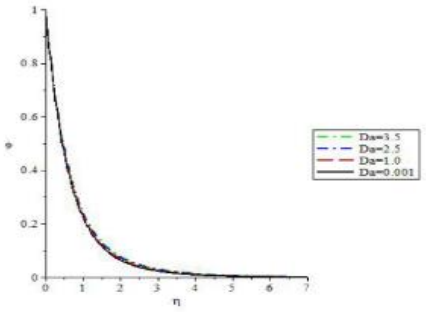

Figure 7: Concentration profile for various values of Da

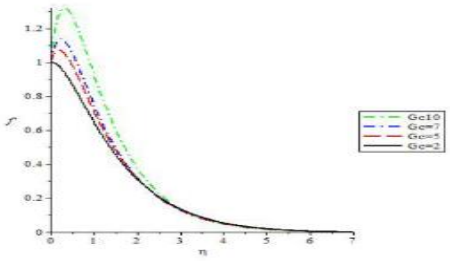

Figure 8: Velocity profile for various values of Gc

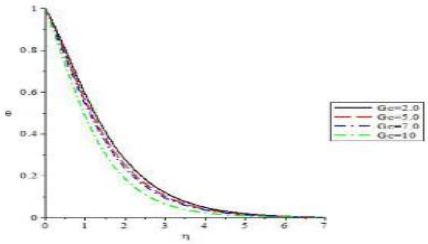

Figure 9: Temperature profile for various values of Gc

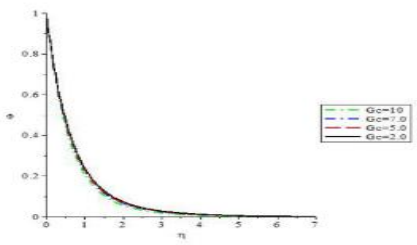

Figure 10: Concentration profile for various values of Gc

In Figs. 8, 9 and 10, exhibit the effects of Gc on the exponential velocity, temperature and concentration respectively. The effect of solutal Grashof number on velocity distribution was illustrated in Fig. 8. It was noticed that increase in Gc led to increase in exponential velocity. The values of temperature and concentration increased with varied

solutal Grashof number. These analyses are true of the Figs. 8, 9 and 10 due to the fact that *Gc* usually increase when one talks about free or natural convection thereby increasing the velocity boundary layer flow. Figs. 11, 12 and 13 exhibit the effects of varied thermal Grashof *Gr* parameter. It was discovered that velocity increased with increase in *Gr* but decrease in temperature and concentration profiles. The implication of this result suggested that slow rate of heat and free convective mass transfer was noticed. In this case, Gr slowed down the exponential temperature and concentration. Figs. 14, 15 and 16 presented the effects of *fw* on the velocity, temperature and concentration profiles respectively. It was discovered that increase in *fw* parameter led to proportional decrease in rate of fluid flow, temperature or heat transfer as well as concentration profile or mass transfer. This parameter has more influence on velocity parameter because it is the parameter that explains the concept of porosity or permeability. The negative values explain the concept of suction while positive values of the parameter reveal the concept of injection. It was observed that suction decreased the exponential velocity, thereby indicating that suction stabilized the boundary layer development. Injection increases the velocity at the boundary layer thereby indicating that injection supports the flow to penetrate more into fluid.

In Fig. 15, it was discovered that temperature decreased as injection decreased, this suggests that injection does not induce cooling hence, fluid transfers to the surface. On the other hand, temperature decreases as suction increases, this means that suction leads to faster cooling of the plates. Fig. 16 represents the fact that concentration decreases as the suction increases and increases as the injection increases due to respective thinner and thickness in mass boundary layer. Figs. 17 to 19 depict the influence of inclination α on the fluid flow, temperature and concentration profiles. The α represents the angular inclination that influences the exponential velocity, temperature and concentration profiles. Fig. 17 showed the effect of α on the velocity profile. Its variation causes fluctuation in fluid flow thereby causing stability at the convergence. In Figs. 18 and 19 it was seen that increase in α parameter causes increase/decrease (sinusoidal representation) in temperature profile. In Fig. 18 the result displays an increased variation of α which in effect led to an increase in concentration profile as well. In essence, the effect of α in the exponential velocity, temperature and concentration thereby explaining the corresponding influence on momentum, energy and mass transfer phenomena.

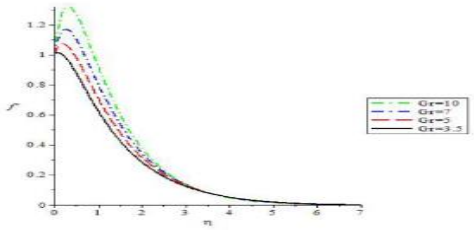

Figure 11: Velocity profile for various values of Gr

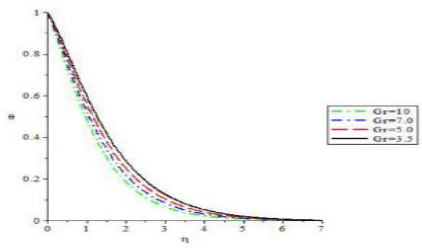

Figure 12: Temperature profile for various values of Gr

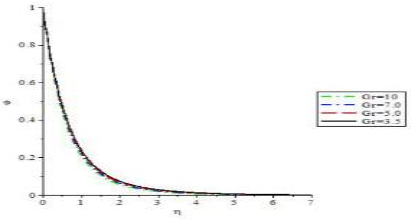

Figure 13: Concentration profile for various values of Gr

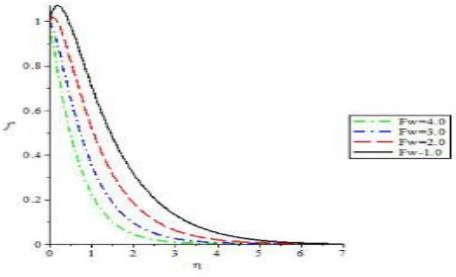

Figure 14: Velocity profile for various values of fw

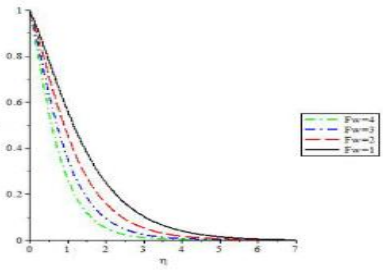

Figure 15: Temperature profile for various values of fw

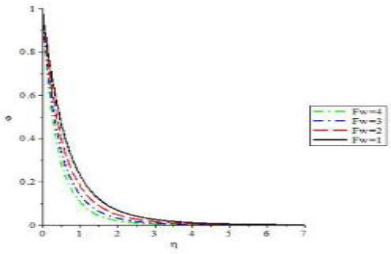

Figure 16: Concentration profile for various values of fw

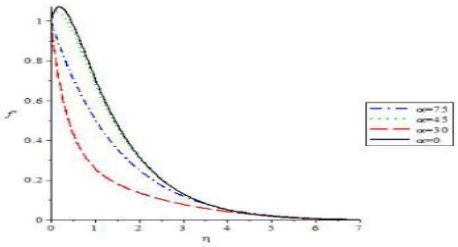

Figure 17: Velocity profile for various values of α

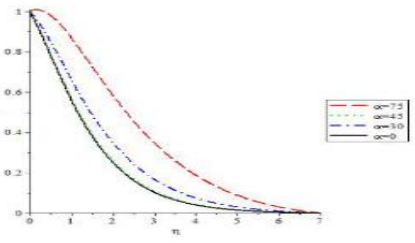

Figure 18: Temperature profile for various values of α

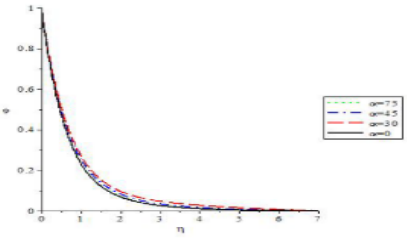

Figure 19: Concentration profile for various values of α

Figures 20 to 22 indicate the effects of radiation on the skin friction, Nusselt number and Sherwood numbers, respectively. It was discovered that increase in radiation parameter, manifest increase in velocity and concentration profiles. It was obvious that velocity and concentration profiles increased with increase in radiation parameter, but decrease in temperature profile. The effects of these were as a result of thickness in the momentum and specie boundary layers. The decrease in thermal temperature was as are sult of thickness in thermal boundary layer. For Figs. 23, 24 and 25, the varied values of Q (independent- heat source parameter) presents the behaviour of skin friction coefficient, Nusselt and Sherwood number. The dimensionless explaining velocity, temperature and concentration were plotted against Q.

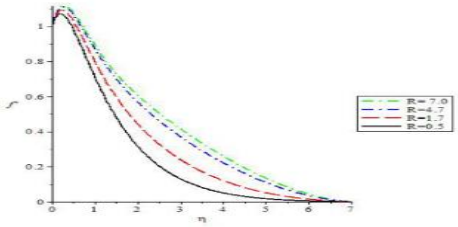

Figure 20: Velocity profile for various values of R

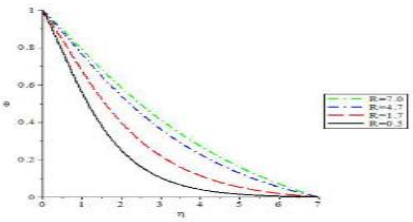

Figure 21: Temperature profile for various values of R

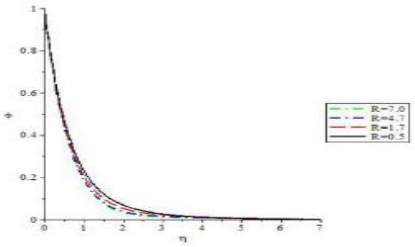

Figure 22: Concentration profile for various values of R

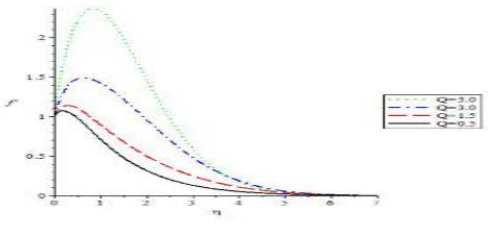

Figure 23: Velocity profile for various values of Q

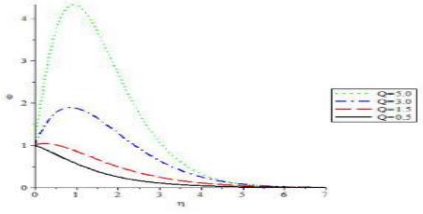

Figure 24: Temperature profile for various values of Q

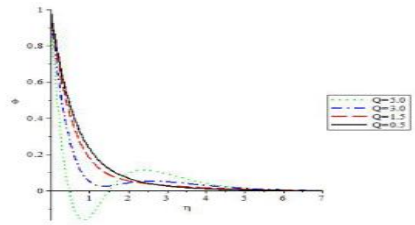

Figure 25: Concentration profile for various values of Q

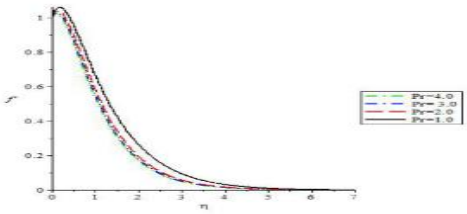

Figure 26: Velocity profile for various values of Pr

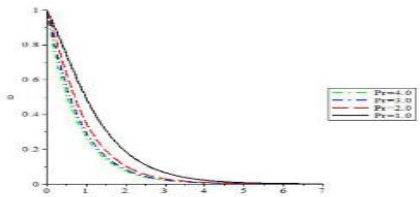

Figure 27: Temperature profile for various values of Pr

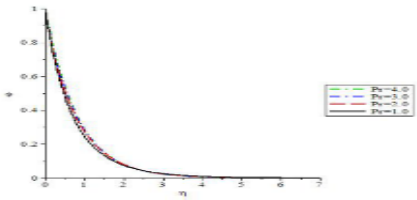

Figure 28: Concentration profile for various values of Pr

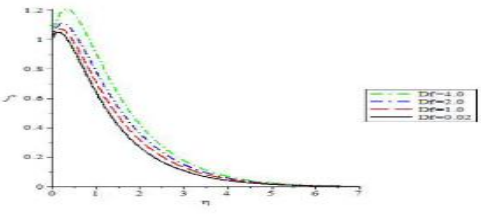

Figure 29: Velocity profile for various values of Df

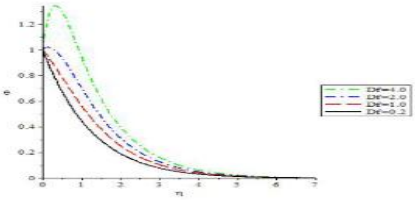

Figure 30: Temperature profile for various values of Df

In Fig. 23 an increase in Q parameter increased fluid flow velocity. In Fig. 24 it could be observed that increase in *Q* parameter led to corresponding change in boundary layer flow. The effect was as a result of heat source or heat sink in the boundary layer on temperature distribution. It was found that variation of Q heat source generates energy which caused the temperature of fluid to increase/decrease. The presence of heat sink in boundary absorbs energy which influenced the temperature of the fluid to increase/decrease, and as it was noticed from the figure the temperature decreased with increase in heat source/sink where $Q > 0$, while it decreased with heat sink $Q < 0$ increasing. In this case heat source/sink were experienced. In Fig. 25, it was observed that increase in Q parameter led to corresponding increase in concentration. In Figs. 26 to 28, the analyses of Pr were presented. Fig. 26 presented the effect of varied Pr on skin friction. An increase in Pr led to decrease in velocity profile. It was discovered that dimensionless velocity or exponential velocity decreased near the surface. Fig. 27 exhibited similar trends. The results shown in Figs. 26 and 27 indicated that *Pr* increased the thickness of thermal boundary layer as a result heat was able to diffuse out of the system, hence temperature profile decreased. Fig. 28 explained that increased in *Pr* decreased the Sherwood number. The outcome of this indicated reduction in diffusivity. Figs. 29, 30 and 31 explained the influence of Dufour parameter when varied with skin friction, Nusselt number and Sherwood numbers respectively the exponential velocity or skin friction increased correspondingly. Fig. 30 showed decrease in exponential temperature while figure 31 showed increase in concentration profile as Dufour parameter increased. Figs. 32 to 34 explained the effects of *Sc* on the velocity, temperature and concentration profiles. Fig. 32 depicted the behaviour of *Sc* on the skin friction coefficient. An increase in *Sc* led to decrease in velocity profile. Fig. 33 explains the increase in *Sc* parameter increased temperature boundary layer. Fig. 34 shows the increase in *Sc* led to decrease in concentration profile. Schmidt number can be defined as the ratio of momentum to the mass diffusivity. It was seen that the velocity and temperature profiles decreased as concentration increased. The *Sc* quantifies the relative effectiveness of momentum and mass transport by diffusion in the hydrodynamic or velocity and concentration boundary layers.

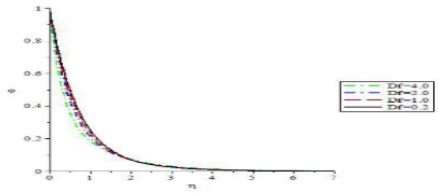

Figure 31: Concentration profile for various values of Df

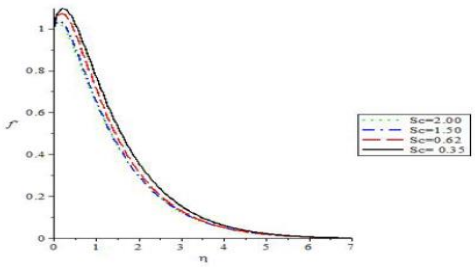

Figure 32: Velocity profile for various values of Sc

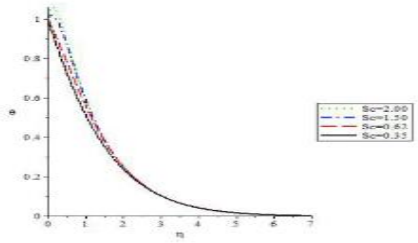

Figure 33: Temperature profile for various values of Sc

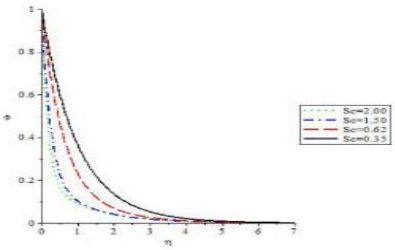

Figure 34: Concentration profile for various values of Sc

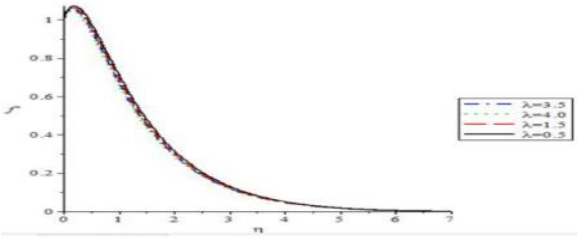

Figure 35: Velocity profile for various values of λ

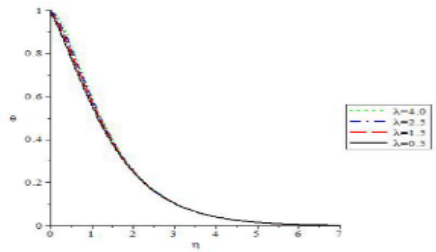

Figure 36: Temperature profile for various values of λ

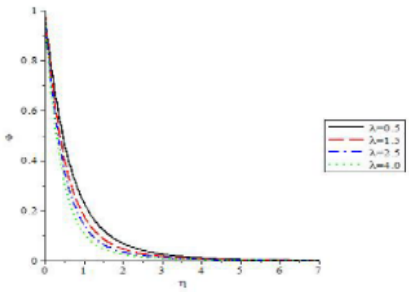

Figure 37: Concentration profile for various values of λ

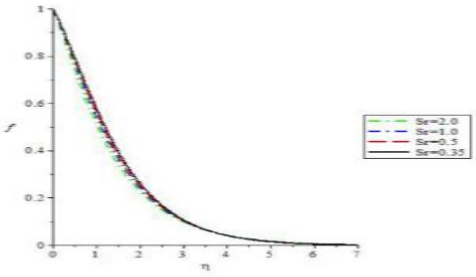

Figure 38: Velocity profile for various values of Sr

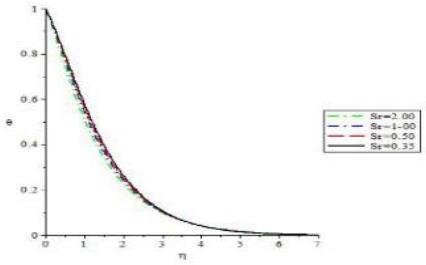

Figure 39: Temperature profile for various values of Sr

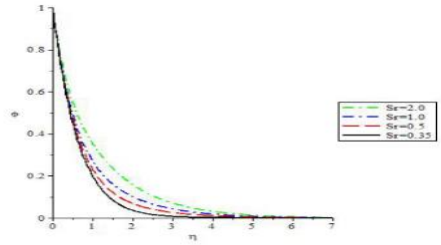

Figure 40: Concentration profile for various values of Sr

Figures 35 to 37 displayed the behaviour of λ and its effects on velocity, temperature and concentration, respectively. As the λ parameter varies increasingly, the skin friction coefficient and Nusselt increased but decreased Sherwood numbers. The clear implication of the plots showed decrease in velocity, temperature and concentration profiles. Figs. 38 to 40 explained the effects of varied Soret parameter on the exponential velocity, temperature and concentration profiles. It was discovered that increase in *Sr.* led to increase in velocity, temperature and specie or concentration distribution. This means that *Sr.* cannot be neglected in explaining fluid flow, heat and mass transfer phenomena. The present results compared favourably with existing literature, similarities/ contrasts were noticed with minimal errors. The reasons for the minimal errors might be due to the method or technique used in solving the problems as well as the parameters we added to the new models solved.

Conclusion

In the present study, cross-diffusion effects involving free convective fluid, heat and mass transfer of MHD fluid in porous media over exponentially stretching sheet was investigated with thermal radiation. The study concluded that solutal Grashof, thermal Grashof, magnetic parameter, radiation parameter, Dufour and Soret numbers had significant effects on MHD fluid flow in porous media stretching surface. This study is recommended for use in plastic extrusion and MHD power generation systems.

References

Alarbi SM, Bazid MAA & El Gendy MS 2010. Heat and mass transfer in MHD visco-elastic fluid flow through a porous medium over a stretching sheet with chemical reaction. *Applied Mathematics*, (1): 446-455.

Ali, M & Alam MS 2014. Soret and Hall Effect on MHD flow, Heat and mass transfer over a Vertical Stretching Sheet in a Porous medium due to Heat generation. *ARPN J. Engr. and Appl. Sci.*, 9(3): 361-371.

Bergman TL, Lavine AS, Incorpera FP &Dewitt DP 2011. *Fundamentals of Heat and Mass Transfer*. New York, USA. John Wiley and Sons, Inc. 7th edition.

Bindi B& Nazar R 2009. Numerical solution of the boundary layer flow over an exponentially stretching sheet with thermal radiation. *Eur. J. Scientific Res.*, 33 (4): 710-717.

Bhattacharyya K 2011. Effects of radiation and heat source/sink on unsteady MHDboundary layer flow and heat transfer over a shrinking sheet with suction/injection. *Frontier Chem. Sci. and Eng.*, 5: 376-384.

Currie IG 2003. *Fundamental Mechanics of Fluids*. Third edition. Mercel Dekkar Inc.

Devi RLVR, Poonimma T, Reddy NB & Venkataramama S 2014. Radiationand mass transfer on MHD boundary layer flow due to an exponentially stretching sheet with heat source. *Int. J. Engr. and Innovative Techn.*, 3(8): 1-14.

Devi RLVR, Neeraja A & Reddy NB 2015. Radiation effect on MHD slip flowpast a stretching sheet with variable viscosity and heat source/sink. *Int. J. Scientific and Innovative Maths. Res.*, 3(5): 8-17.

Douglas JF, Gariosok JM, Swaffield JA & Jack BJ 2005. *Fluid Mechanics*. Harlow, England. Pearson Education Limited.

Eckert ERG & Drake RM 1972. *Analysis of heat and mass transfer*, McGrawHill, New York.

Eegunjobi AS 2013. *Analysis of laminar flow, thermal stability and entropy generationin porous channel*. PhD thesis, Cape Peninsula university of Technology.

Elbeshbeshy EMA 2001. Heat transfer over an exponentially stretching continuous surface with suction. *Archives Mechanics*, 53: 643-651.

Ibrahim SM & Suneetha K 2015. Effect of heat generation and thermal radiation on MHD flow near a stagnation point on a linear stretching sheet in porousmedium and presence of variable thermal conductivity and mass transfer. *Journalof Comp. and Appl. Res. Mech. Engr.* 4(2): 133-144.

Ibrahim SY & Makinde OD 2010. Chemically reacting MHD boundary layer flowof heat and mass transfer over a moving plate with suction. *Scientific Research and Essays*, 5(9): 2875-2882.

Irogham DB & Pop I (Ed.) 2005. *Transport Phenomena* (1) Elsevier, Oxford.

Ishak A 2011. MHD boundary layer flow due to an exponentially stretching sheet with radiation effects. *Sain Malaysiana* 40(4): 391-395.

Ishak A, Nazar R & Pop I 2007. Magnetohydrodynamic stagnation point flow towards as tretching vertical sheet in a micropolar fluid. *Magnetohydrodynamics*, 43: 83-97.

Jain MK, Iyengar, SRK & Jain RK 1985. *Numerical Methods for Scientific and Engineering Computation*, Wiley Eastern Ltd., New Delhi, India.

Kala BS, Singh M & Kumar A 2014. Steady MHD free convective flow andheat transfer over nonlinearly stretching sheet embedded in an extended DarcyForcheimmer porous medium with viscous dissipation. *J. Global Res. Math. Achives*, 1-5.

Kreith F, Mangluk RM & Bohn MS 2011. *Principles of Heat Transfer*, Cengage Learning Inc., Oregon, U.S.A.

Kreyszig E 2006.*Advanced Engineering Mathematics*, 9th edition. Wiley (ed) Singapore.

Lakshmi Narayana PA & Murthy PVSN 2007. Soret and Dufour effects in adoubly stratified Darcy porous medium. *Journal of Porous Media*, 10: 613-624.

Lakshmi MP, Reddy NB & Poornima T 2012. MHD boundary layer flow of heat and mass transfer over a moving vertical plate in a porous medium with suction and Viscous Dissipation. *Int. J. Engr. Res. Applic.*, 2(5): 149-159.

Makinde OD 2010. On MHD heat and mass transfer over a moving vertical plate with a convective surface boundary condition. *The Canadian J. Chemical Engr.*, 88(6): 983-990.

Mukhopadhyay S 2012. Slip effects on MHD boundary layer flow over an exponentially stretching sheet with suction/blowing and thermal radiation. *Ain. Shams Engineering Journal*, 2: 20-22.

Nalinakshi N, Dinesh PA & Chandrashekar DV 2013. Effect of variable fluid properties and MHD on mixed convection heat transfer from a vertically heated plate embedded in a sparsely packed porous Medium. *IOSR Journal of Mathematics*, 7(1): 20-31

Nield DA & Bejan A 2006. *Convection in Porous Media*, 3rd Edition. Springer Verlag, New York.

RamReddy C& Srinivasacharya D 2012. Soret and Dufour effects on mixed convection from an exponentially stretching surface in non-Darcy porous medium. *International Conference on Fluid Dynamics and Thermodynamics Technologies* [IACSIT Press, Singapore], 33: 43-48.

Sajid M & Hayat T 2008. Influence of thermal radiation on the boundary layer flow due to an exponentially stretching sheet. *International Communication Heat Mass Transfer*, 35:347-356.

Srivas M& Kishan N 2015. Unsteady MHD flow and heat transfer of nanofluid over a permeable shrinking sheet with thermal radiation and chemical reaction. *Am. J. Engr. Res.*, 4(6): 68-79.

Sharma PR, Sharma M & Yadav RS 2014. Viscous dissipation and mass transfer effects on unsteady MHD free convective flow along a moving vertical porous plate inthe presence of internal heat generation and variable suction. *Int. J. Sci. and Res. Public.*, 4(9): 1-9.

Sharma PK 2004. Unsteady effect on MHD free convective and mass transfer flowthrough porous medium with constant suction and constant heat transfer past asemi-infinite vertical porous plate. *Journal of Computational Materials and Science*,40: 186-192.

Shankar B, Prabhakar Reddy B & Ananda Rao J 2010. Radiation and mass transfer effects on MHD free convection fluid flow embedded in a porous medium with heat generation/absorption. *Indian J. Pure and Appli. Phy.*, 48: 157-165.

Shekhar KVC 2014 Boundary layer Phenomena of MHD flow and Heat transfer over an exponentially stretching sheet embedded in a thermally stratified medium. *Int. J. Sci., Engr. and Techn. Res.*, 3(10): 2715-2721.

Sibanda P, Khidir & Awad H 2012. On Cross-diffusion effects on flow over a verticalsurface using linearization method in boundary layer problem. *Open Journal*, 25.

Soret C1880. Influence de la temperature sur la distribution des sels dans leurs solutions. *C.R. Academy of Science*, Paris, 91: 289-291.

Srinivasacharya D & RamReddy C 2011. Mixed convection from an exponentially stretching surface with Soret and Dufour effects. *IEEE proceedings of 2011 World Congress on Engr. and Techn*. China, 2: 707-711.

Srinivasacharya D & RamReddy C 2011. Soret and Dufour effects on mixed convection from an exponentially stretching surface. *Int. J. Nonlinear Sci.*, 12: 60-68.

Srinivasacharya D & RamReddy C 2012. Mixed convection heat and mass transfer in a micropolar fluid with Soret and Dufour effects. *Advanced Appl. Maths. and Mech.*, 3: 389-400.

Srinivasacharya D & RamReddy C 2013. Cross-diffusion effects on mixed convection from an exponentially stretching surface in non-Darcy porous medium. *Heat Transfer - Asian Journal* (Wiley), 1-14.

Srinivasacharya D, Pranitha J & RamReddy C 2012. Magnetic and double dispersion effects on free convection in a non-Darcy porous medium saturated with power-law fluid. *Int. J. Comp. Methods in Engr., Sc. and Mech.*, 13: 210-218.

Subhakar MJ & Gangadhar K 2012. Soret and Dufour effects on MHD free convection heat and Mass Transfer flow over a stretching vertical plate with suction and heat source/sink. *Int. J. Modern Engr. Res*., 2(5): 3458-3468.

Sulochana C & Kumar MKK 2015. Nonlinear thermal radiation and chemical reaction effects on MHD 3D Casson fluid flow in porous medium *Chem. and Process Engr. Res.*, 37: 24-34.

Sundaram V, Balasubramanian R & Lakshminarayanan KA 2003. *Engineering Mathematics*. 3, VIKAS Publishing House LTD, New Delhi, 173.

Stroud KA 1996. *Engineering Mathematics*. Third Edition. London Macmillan Press Limited.

Stroud KA & Booth DJ 2003. *Engineering Mathematics*. Fourth Edition. London Macmillan Press Limited.

Turkyilmazoglu M 2012. Exact analytical solutions for heat and mass transfer of MHD slip flow in nanofluids, *Chem. Engr. Sci.*, 84: 182-187.

Vafai P 2005. *Handbook of porous media. Second edition*. New York, Taylor and Erancis.

Vasdasz P 2008. *Emerging Topics in Heat and Mass Transfer in porous Media*. New York Springer.